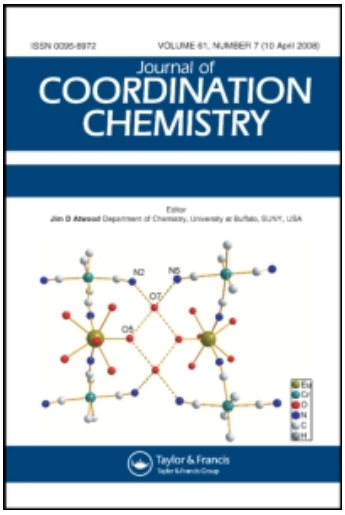

Journal of Coordination Chemistry
Publication details, including instructions for authors and subscription information:
http://www.informaworld.com/smpp/title~content=t713455674

Synthesis, characterization, and biological studies of lanthanide complexes with 2,6-pyridine dicarboxylic acid and α-picolinic acid

Dongfang Xu[a]; Yanming Xu[a]; Ningning Cheng[a]; Xianan Zhou[a]; Yang Shi[a]; Qizhuang He[a]
[a] College of Life and Environment Sciences, Shanghai Normal University, Shanghai 200234, China

First published on: 13 July 2010

To cite this Article Xu, Dongfang , Xu, Yanming , Cheng, Ningning , Zhou, Xianan , Shi, Yang and He, Qizhuang(2010) 'Synthesis, characterization, and biological studies of lanthanide complexes with 2,6-pyridine dicarboxylic acid and α-picolinic acid', Journal of Coordination Chemistry, 63: 13, 2360 — 2369, First published on: 13 July 2010 (iFirst)
To link to this Article: DOI: 10.1080/00958972.2010.499937
URL: http://dx.doi.org/10.1080/00958972.2010.499937

Journal of Coordination Chemistry
Vol. 63, No. 13, 10 July 2010, 2360–2369

Taylor & Francis
Taylor & Francis Group

Synthesis, characterization, and biological studies of lanthanide complexes with 2,6-pyridine dicarboxylic acid and α-picolinic acid

DONGFANG XU, YANMING XU, NINGNING CHENG, XIANAN ZHOU, YANG SHI and QIZHUANG HE*

College of Life and Environment Sciences, Shanghai Normal University, Shanghai 200234, China

(*Received 6 January 2010; in final form 22 April 2010*)

Four new solid ternary complexes of lanthanide with 2,6-pyridine dicarboxylic acid and α-picolinic acid $[Ln(DPA)(L^{\alpha})(H_2O)]\cdot 2H_2O$ ($Ln = La^{3+}$, Ce^{3+}, Eu^{3+}, or Gd^{3+}; DPA = 2, 6-pyridine dicarboxylic acid; HL^{α} = α-picolinic acid) have been synthesized and characterized by elemental analysis, molar conductance, FT-IR, UV–Vis, and TG–DTA. The antibacterial activities indicate that all the complexes exhibit antibacterial ability against *Escherichia coli* and *Staphylococcus aureus* with broad antimicrobial spectra. The anticancer activity of the La complex against K562 tumor cell *in vitro* is measured using methyl thiazolyl tetrazolium (MTT) colorimetry and flow cytometry. The La complex can induce K562 tumor cell apoptosis, presenting the best apoptosis effect by acting on the S period after inducing K562 tumor cell for 72 h.

Keywords: Lanthanide complex; Apoptosis; Antitumor; Antibacterial

1. Introduction

Considerable attention has been paid to study metal complexes with antibacterial, and antitumor activities and interactions between biological macromolecules [1, 2]. Lanthanide complexes have received attention due to a wide field of applications [3–6]. Some lanthanide complexes are biological probes for medical diagnosis and drug development [7]. Many probes for DNA analysis have been proposed [3, 8, 9]. Recently, it has been shown that some lanthanide complexes might have a potential role in the treatment of tumor cell lines [10]. Lanthanide complexes have inspired many efforts on the design and synthesis as potential anticancer and antibacterial agents because of their special electronic configuration [11–16].

Metal or ligands can be varied in an easily controlled way to facilitate individual applications [17] and the study of lanthanide complexes with organic ligands has received considerable attention [18, 19]. Pyridine has good bioactivity [20, 21] and 2,6-pyridine dicarboxylic acid (DPA) has special biological activity in itself

*Corresponding author. Email: hqz@shnu.edu.cn

Journal of Coordination Chemistry
ISSN 0095-8972 print/ISSN 1029-0389 online © 2010 Taylor & Francis
DOI: 10.1080/00958972.2010.499937

and its complexes. For example, complexes of gallium showed notable and higher antibacterial activity than free ligand [22] and complexes of iron were recognized as specific molecular tools in DNA cleavage [23, 24]. DPA and α-picolinic acid (HL^{α}) have practical importance in biology due to the presence of several potential N, O donors, which inhibit the growth of bacteria [25]. Those containing N=C–C=N form a strong chelated ring giving delocalization associated with extended conjugation. They can yield mono or polynuclear complexes [26–28]. These advantages encourage us to choose DPA and HL^{α} as ligands and synthesize complexes with antibacterial and antitumor properties. Because of the importance of lanthanide complexes and our interest in the synthesis of lanthanide complexes [16, 18, 29], we report herein the synthesis, spectroscopic studies, thermal investigation, and biological activities of lanthanide complexes with DPA and HL^{α}, in continuation of our research to develop new anticancer and antibacterial agents in biological activities for lanthanide complexes and other related fields.

2. Experimental

2.1. *Materials*

Ln_2O_3 (99.99%) were purchased from Yue Long Chemical Plant (Shanghai). DPA and α-picolinic acid were purchased from J&K Chemical Ltd. RPMI 1640 and tetrazolium salt 3-(4,5-dimethylthiazol-2-yl)-2,5-diphenyltetrazolium bromide (MTT) were purchased from Sigma. Fetal calf serum (FCS) was purchased from GIBCO. All reagents were of analytical grade and used without purification.

2.2. *Bacterium and cell*

Staphylococcus aureus (*S. aureus ATCC6358P*) and *Escherichia coli* (*E. coli ATCC11229*) were provided by Shanghai Drug Institute, Chinese Academy of Sciences. Human leukemia K562 cells were obtained from Cell Bank of Chinese Academy of Sciences (Shanghai, China).

2.3. *General measurements*

C and H analyses were performed on an Elementar Vario EL III elemental analyzer; the percentages of the lanthanide were determined by complexometric titration with EDTA. Infrared spectra were measured at room temperature on a PK-60000 FT-IR using KBr pellets from 4000–400 cm^{-1}. UV spectra were recorded on a Perkin Elmer17. TG–DTA curves were recorded on a thermal oflex DTA derivatograph at a rate of 10 K min^{-1} with samples heating in ambient atmosphere by Perkin-Elmer Pyris Diamond. Fluorescence spectra were recorded with a Cary-E fluorescence spectrophotometer.

2.4. *Synthesis of complexes*

The complexes were prepared in the following steps. In the first step, lanthanide chloride was prepared by dissolving Ln_2O_3 in hot hydrochloric acid, evaporating to syrup, and diluting with ethanol to a desired volume. 5 mmol L^{-1} DPA and 10 mmol L^{-1} NaOH were dissolved in 50 mL distilled water. Subsequently, 5 mmol L^{-1} $LnCl_3$ was added to the above-mentioned system, adjusting pH to 6, stirred and refluxed for 3 h in a water bath. Then, 5 mmol L^{-1} HL^{α} solution was added dropwise, keeping pH at 6, stirred and refluxed for 6 h. The resulting solution was filtered, washed with distilled water three times, and then dried in a vacuum oven. Four rare earth complexes with DPA and HL^{α} were synthesized using this method.

2.5. *Test of antibacterial activity*

The antibacterial activity of the ligands and complexes were tested by disc diffusion and nutrition broth dilution method.

2.5.1. Method of paper disc diffusion. Complexes, $LnCl_3$, and the ligands (0.005 mol L^{-1}) were prepared and the antibacterial activity of all the compounds against *S. aureus* and *E. coli* was studied. The bacterium suspension concentration was controlled as 5×10^5–5×10^6 cfu mL^{-1}; diameters of filter paper were 5 mm, and for the experiments, flat plates were incubated at 37°C (bacterium) for 18 h. Their inhibition diameter (including filter paper) was measured with a vernier caliper [29].

2.5.2. Method of nutrition broth dilution. To quantitatively understand antibacterial activities, the antibacterial activity of the complex was evaluated for its minimum inhibitory concentration (MIC) by the microdilution broth method [29]. Sample solutions were added to broth for different concentrations. Samples of each bacterial suspension were added to the serial dilution of the test substances. The inoculated test tubes were incubated at 37°C under aerobic conditions. After 24 h, the turbidity was evaluated. The MIC was defined as the lowest antimicrobial concentration of the test samples. The experiments were repeated three times and the results expressed in average values.

2.6. *Test of antitumor activity*

2.6.1. Morphological observation of apoptosis. Morphological observation of the La complex inducing apoptosis of leukemia K562 cells was carried out on a fluorescence microscope after collecting 30 μL of the treated leukemia K562 cells and staining with 10 μL of acridine orange (AO).

2.6.2. Antitumor activity. The antitumor activities [29] of the La complex on leukemia K562 cells were tested using the MTT (3-(4,5-dimethylthiazol-2-yl)-2,5-diphenyltetrazolium bromide) method and fluorescence-activated cell sorting (FACS). Briefly, 1×10^5 mL^{-1} leukemia K562 cells and each compound at various concentrations were

put into 1 mL medium and were then added to each well of a 96-well plate. Tests at each concentration were conducted in eight holes. The plate was incubated at 37°C in a humidified atmosphere containing 5% CO_2 for 44 h. MTT solution (10 μL) was then added to each well. After the plate was further incubated for 4 h, 100 μL 10% SDS was added to each well to solubilize formazan dye. The optical density (OD) at 570 nm was read by an enzyme-linked immunosorbent assay (ELISA) reader the next day. The mean and standard deviation of each group were calculated.

$$\text{Inhibitory rate (IR, \%)} = (1 - \text{OD}_{\text{complex}}/\text{OD}_{\text{blank}}) \times 100\%.$$

Similarly, $1 \times 10^5\,\text{mL}^{-1}$ leukemia K562 cells and the La complex at various concentrations were put into 1 mL medium and were incubated at 37°C in a humidified atmosphere containing 5% CO_2 before testing by flow cytometry.

3. Results and discussion

3.1. *Elemental analysis and molar conductivity*

The Ln(III) percentage was determined by complexometric titration with EDTA, according to the method described by He [29]. Analytical data of Ln(III), C, H, and N percentages (found/calculated) for the complexes are listed in table 1. Molar conductivity of the four complexes in DMSO ($1 \times 10^{-3}\,\text{mol L}^{-1}$) at room temperature showed that they are non-electrolytes in DMSO [30].

3.2. *FT-IR spectra*

Some results of IR spectra are given in table 2. Comparing IR spectra of complex with DPA and HL^{α}, we conclude that the absence of the COO^- group of DPA and HL^{α} at 1699 and 1592 cm^{-1} suggest coordination of COO^- with the lanthanide ions. Two new bands at about 1658 and 1440 cm^{-1} can be attributed to the asymmetric and symmetric stretching vibrations, respectively. According to Deacon and Philips and Taylor *et al.* [31, 32], if the separation value ($\Delta = \nu_{as} - \nu_s$) in lanthanide carboxylates is lower than that of Na^+ carboxylate, coordination is mainly bidentate chelating, bidentate bridging, or tridentate chelating bridging. The separation values ($\Delta = \nu_{as} - \nu_s$) between ν_{as}(COO) and ν_s(COO) peaks is about 218 cm^{-1} in the complexes, which is lower than that in DPA (290 cm^{-1}) and larger than that of HL^{α} (210 cm^{-1}), which show that the carboxylate is bidentate chelating with lanthanide ions for DPA and monodentate chelating for HL^{α}. Bands at 1575, 646, and 418 cm^{-1} are attributed to the $\delta_{8a\text{ or }8b}$, δ_{6a}, and δ_{16b} of the pyridine ring of DPA, respectively, and that of HL^{α} at 1530, 679,

Table 1. Elemental analyses and molar conductivity data of complexes.

Complexes	Ln (%)	C (%)	H (%)	N (%)	Λ_m
$[La(DPA)(L^{\alpha})(H_2O)] \cdot 2H_2O$	29.13 (28.93)	32.88 (32.49)	2.68 (2.71)	6.11 (5.83)	20.8
$[Ce(DPA)(L^{\alpha})(H_2O)] \cdot 2H_2O$	29.25 (29.11)	32.72 (32.41)	2.67 (2.70)	6.02 (5.82)	19.2
$[Eu(DPA)(L^{\alpha})(H_2O)] \cdot 2H_2O$	30.72 (30.81)	31.87 (31.63)	2.58 (2.64)	5.78 (5.68)	16.7
$[Gd(DPA)(L^{\alpha})(H_2O)] \cdot 2H_2O$	31.38 (31.55)	31.65 (31.30)	2.54 (2.61)	5.74 (5.62)	14.3

and 420 cm^{-1}. Shifting to higher frequency, 1592, 699, and 426 cm^{-1} in the complex indicate that nitrogen of pyridine took part in coordination of the lanthanide ions. Furthermore, IR spectra shows a strong and broad band at 3350 cm^{-1}, ascribed to the stretching vibration of the crystal water.

3.3. *UV–Vis spectra*

UV–Vis spectra of the four complexes, DPA, and α-picolinic acid were measured at 1×10^{-4} mol L^{-1} using DMSO as solvent (Supplementary material). The ε_{max} of the ternary complexes are different from that of the free ligands, which indicates formation of new complexes.

Absorption bands of DPA and α-picolinic acid, attributed to $\pi \rightarrow \pi^*$ transition of conjugated system, were found at 269 and 264 nm, respectively. However, the $\pi \rightarrow \pi^*$ transition of α-picolinic acid had a bathochromic shift while that of DPA had a violet shift when the complexes formed. The overlapping of the two absorption bands formed a new one of the ternary complexes, which also indicated the formation of new complexes [33].

3.4. *TG–DTA*

The TG–DTA curves of the four ternary complexes are similar when heated in air from 25°C to 1000°C (table 3). The complexes show three steps, the first corresponding to loss of two crystal waters from 100°C to 110°C (endothermic). The second corresponds to loss of coordinated water from 170°C to 260°C, in agreement with IR and elemental analysis data. The anhydrous complexes decompose to oxides accompanied by a strong exothermic effect with a single peak from 500°C to 600°C. The oxides are stable at temperature 600°C.

Based on the above-mentioned studies, we propose a tentative coordination structure for the complexes as shown in scheme 1.

Table 2. IR data of ligands and complexes.

		Ligands (cm^{-1})		Complexes (cm^{-1})			
Groups	Types	DPA	HL^{α}	La^{3+}	Ce^{3+}	Eu^{3+}	Gd^{3+}
COOH	$\nu_{(C=O)}$	1699	1592	–	–	–	–
COO^-	$\nu_{as(OCO)}$	1707	1612	1658	1657	1654	1655
	$\nu_{s(OCO)}$	1417	1402	1438	1440	1433	1432
	$\Delta_{\nu as-\nu s}$	290	210	220	217	221	223
	$\delta_{8a \text{ or } 8b}$	1575	1530	1592	1591	1589	1588
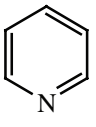	δ_{6a}	646	679	698	687	695	694
	δ_{16b}	418	420	426	425	420	425
H_2O	ν_{OH}	–	–	3343	3340	3358	3349

Table 3. TG–DTA data of the complexes.

Complexes	Endothermic peak of dehydration (°C)	Endothermic peak of decomposition (°C)		Weight loss (%)
		I	II	
$[La(DPA)(L^{\alpha})(H_2O)]\cdot 2H_2O$	99.58, 173.69	472.19	496.03	57.76 (59.57)
$[Ce(DPA)(L^{\alpha})(H_2O)]\cdot 2H_2O$	101.42, 185.58	471.59	505.04	56.63 (59.42)
$[Eu(DPA)(L^{\alpha})(H_2O)]\cdot 2H_2O$	98.33, 178.27	450.38	–	54.97 (58.00)
$[Gd(DPA)(L^{\alpha})(H_2O)]\cdot 2H_2O$	97.69, 165.77	442.29	–	53.06 (57.38)

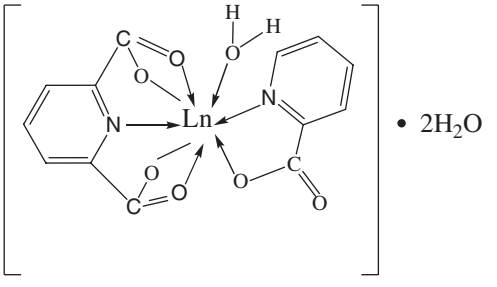

Scheme 1. Tentative coordination structure for the complexes.

3.5. *Antibacterial activity*

The antibacterial activities of the complexes, $LnCl_3$, and the ligands are evaluated using the paper disc diffusion method and the nutrition broth dilution method against *E. coli ATCC11229* and *S. aureus ATCC6358P*. Penicillin (North China Pharmaceutical Co. Ltd, D0211107, Hebei 050015, China) was used as standard drug for bacteria. The diameter of growth inhibition area was 17 and 56 mm against *E. coli* and *S. aureus*, respectively. The MIC of penicillin was 150 and 1.6 $\mu g\,mL^{-1}$ against *E. coli* and *S. aureus*, respectively, (omitted in table 4).

The results in the forms of the diameter of growth inhibition (mm) and the MIC ($\mu g\,mL^{-1}$) are given in table 4. Figure S1a and S1b (Supplementary material) show the diameter of the growth inhibition area of $[La(DPA)(L^{\alpha})(H_2O)]\cdot 2H_2O$ against *E. coli* and *S. aureus*, respectively. The antibacterial results are summarized as follows: (1) All the tested lanthanide ternary complexes exhibit antibacterial activities against *E. coli* and *S. aureus*. (2) The antibacterial activities of the complexes are better than either free ligand. (3) The La complex shows favorable antibacterial activity with the diameter of growth inhibition area (17, 15 mm) and the MIC (400, 450 $\mu g\,mL^{-1}$) against *E. coli* and *S. aureus* among the four complexes.

The increase in antibacterial activity of the complex may be due to the effect of the metal ion on the normal cell process. Complexation considerably reduces the polarity of the metal ion because of partial sharing of its positive charge with the donor groups. The π-electron delocalization in this chelating ring also increases the lipophilic nature of the central metal atom, which subsequently favors its permeation through the lipid layers of cell membrane [1, 25, 34].

Table 4. Antibacterial activity expressed as diameter of growth inhibition area (Panel A) and MIC (Panel B).

Complex	Concentration ($mol\,L^{-1}$)	Bacterial strain	
		E. coli ATCC11229	*S. aureus ATCC6358 P*
Panel A: Diameter of growth inhibition area (mm)			
$[La(DPA)(L^{\alpha})(H_2O)]\cdot 2H_2O$	0.005	17	15
$[Ce(DPA)(L^{\alpha})(H_2O)]\cdot 2H_2O$	0.005	16	15
$[Eu(DPA)(L^{\alpha})(H_2O)]\cdot 2H_2O$	0.005	14	14
$[Gd(DPA)(L^{\alpha})(H_2O)]\cdot 2H_2O$	0.005	13	13
DPA	0.005	10	10
HL^{α}	0.005	5	5
$ReCl_3$	0.005	0	0
Panel B: MIC ($\mu g\,mL^{-1}$)			
$[La(DPA)(L^{\alpha})(H_2O)]\cdot 2H_2O$		400	450
$[Ce(DPA)(L^{\alpha})(H_2O)]\cdot 2H_2O$		410	450
$[Eu(DPA)(L^{\alpha})(H_2O)]\cdot 2H_2O$		460	470
$[Gd(DPA)(L^{\alpha})(H_2O)]\cdot 2H_2O$		480	500
DPA		700	750
HL^{α}		>800	>800
$LnCl_3$		>800	>800

3.6. *Morphological observation of apoptosis*

Based on the above-mentioned results, we choose the La complex as the model complex to test anticancer activity. The morphological observation of apoptosis of La complex is shown in figure 1. When AO enters the cancer cells, the DNA exhibits green fluorescence and RNA exhibits orange fluorescence. Fifteen minutes later, the control cells and the apoptosis are observed on a fluorescent microscope. We conclude that the La complex induces apoptosis of leukemia K562 cells.

3.7. *Assessment of cytotoxicity using the MTT method*

In order to investigate the anticancer activity of La complex and compare it with the ligands, they are all made to react with K562 cancer cells by the MTT method. The inhibitory rate of the La complex is calculated based on the absorption rate, as listed in table 5.

The La complex ($\geq 0.01\,\mu g\,mL^{-1}$) inhibited proliferation of cancer cell by 32.68%. At $1\,\mu g\,mL^{-1}$, the inhibitory rate was 48.28%. The ligands did not differ significantly from the complex in the cytotoxicity pattern. At concentration of $0.01\,\mu g\,mL^{-1}$, the inhibitory rate of $LaCl_3$, DPA, and HL^{α} was 5.09%, 22.15%, and 21.07%, respectively. When the concentration was increased to $1\,\mu g\,mL^{-1}$, the inhibitory rate of $LaCl_3$, DPA, and HL^{α} was 11.02%, 37.28%, and 38.47%, respectively. According to the inhibitory rate, the complex was more toxic to K562 cancer cells than the ligands.

The complex possessing antitumor activities may be attributed to the extended planar structure induced by conjugation from the chelation of the rare ion with the ligands [35].

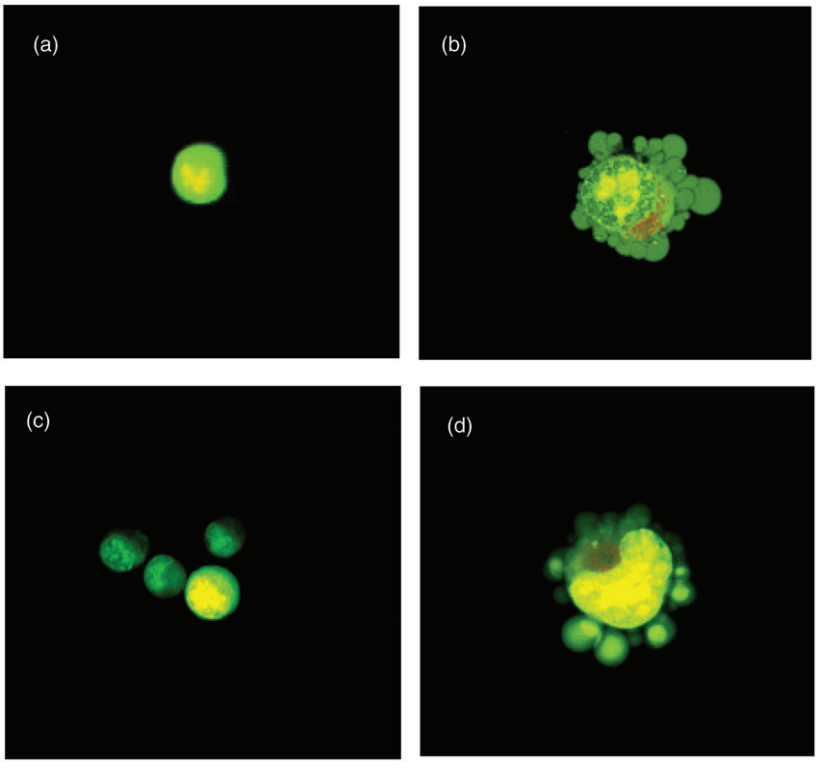

Figure 1. Leukemia K562 cells observed under the fluorescence microscope: (a) control; (b)–(d) apoptotic.

Table 5. Inhibitory rate of ligands and La complexes of different concentration on K562 cells for 48 h.

	Inhibitory rate (%)			
Groups ($\mu g\,mL^{-1}$)	$LaCl_3 \cdot 6H_2O$	HL^{α}	DPA	La complex
DMSO	8.77	8.77	8.77	8.77
0.01	5.09	22.15	21.07	32.68
0.1	9.47	34.71	31.93	43.53
1	11.02	37.28	38.47	48.28
10	20.38	35.72	36.85	46.39

3.8. *Fluorescence-activated cell sorting*

The results of FACS tested for La complex inducing the apoptosis of leukemia K562 cells for 48 h shown in Supplementary material indicate that the La complex has remarkable effect on inducing the apoptosis of leukemia K562 cells. The best effect is found at $1\,\mu g\,mL^{-1}$, which is better than the free ligands at the same concentration.

Table 6. FACS testing for numerical value of cell period (%).

Groups	24 h	48 h	72 h	96 h
G0–G1 (%)	38.04	39.45	45.60	35.09
G2–M (%)	17.45	22.13	22.05	15.41
S (%)	44.51	38.42	32.35	49.50

When the La complex induces apoptosis of leukemia K562 cells for 24–72 h, the ratio of cells in G0–G1 (first gap) period increased while that in S (synthesis) period decreased, indicating that the La complex affects the number of cells in G1 period and prolongs the time of the proliferous cells in S period, reducing the number of cells switching from S period to G2 (second gap)–M (mitosis) period. As the ratio of cells in S period is found increasing obviously in human cancer, the results of FACS indicate that 1 μg mL^{-1} of the La complex presents the best apoptosis effect after inducing K562 tumor cells for 72 h, acting on the S period. When the inducing time is extended to 96 h, the ratio of cells in G0–G1 period decrease while that in S period increase, indicating that cells have turned into the period of drug tolerance [36, 37] (table 6).

4. Conclusion

Four ternary lanthanide complexes were prepared and characterized, which exhibit better inhibitory effects on *E. coli* and *S. aureus* than the free ligands. The La complex exhibits stronger inhibitory effect on leukemia K562 cells than the free ligands. Some studies revealed that some lanthanide complexes are potent cytotoxic agents [10]. At concentration of 1 μg mL^{-1}, the La complex presents the best apoptosis effect acting on the S period after inducing K562 tumor cell for 72 h.

Acknowledgments

We are grateful to Leading Academic Discipline Project of Shanghai Normal University (DZL806), the National Nature Science Foundation of China (20671063), Shanghai Key Discipline Construction Project (S30406), the Key Subjects of Shanghai Normal University (DZL711), and the research of Shanghai Normal University (SK200829) for the financial support.

References

[1] Y.L. Song, Y.T. Li, Z.Y. Wu. *J. Inorg. Biochem.*, **102**, 1691 (2008).
[2] S. Dhar, M. Nethaji, A.R. Chakravarty. *J. Inorg. Biochem.*, **99**, 805 (2005).
[3] S.V. Eliseeva, J.-C.G. Bünzli. *Chem. Soc. Rev.*, **39**, 189 (2010).
[4] E.J. Werner, A. Datta, C.J. Jocher, K.N. Raymond. *Angew. Chem., Int. Ed.*, **47**, 8568 (2008).

[5] P. Hermann, J. Kotek, V. Kubicek, I. Lukes. *Dalton Trans*., 3027 (2008).
[6] M. Woods, D.E. Woessner, A.D. Sherry. *Chem. Soc. Rev*., **35**, 500 (2006).
[7] A.-L. Gassner, C. Duhot, J.-C.G. Bünzli, A.-S. Chauvin. *Inorg. Chem*., **47**, 7802 (2008).
[8] J.L. Worlinsky, S. Basu. *J. Phys. Chem. B*, **113**, 865 (2009).
[9] T. Nishioka, J. Yuan, Y. Yamamoto, K. Sumitomo, Z. Wang, K. Hashino, C. Hosoya, K. Ikawa, G. Wang, K. Matsumoto. *Inorg. Chem*., **45**, 4088 (2006).
[10] I. Kostova, T. Stefanova. *J. Coord. Chem*., **62**, 3187 (2009).
[11] J.Z. Ni. *Bioinorganic Chemistry of Rare Earth*, p. 288, Science Press, Beijing (2002).
[12] Y.T. Yang. *Spectrochim. Acta, Part A*, **55**, 1527 (1999).
[13] R.M. Supkowski, J.P. Bolender, W.D. Smith, L.E.L. Reynolds, W.D. Horrocks. *Coord. Chem. Rev*., **186**, 307 (1999).
[14] R. Yang, S.Y. He, A.P. Gu, Z.Y. Wen, X. Lin, H.Z. Wen. *Acta Phys. Chim. Sin*., **19**, 610 (2003).
[15] Y.B. Wang, J.H. Yang, X. Wu, L. Li, S. Sun, B.Y. Su, Z.S. Zhao. *Anal. Lett*., **36**, 2063 (2003).
[16] H. Yu, Q.Z. He, J. Yang, W.J. Zheng. *J. Rare Earths*, **24**, 4 (2006).
[17] X.L. Wang, H. Chao, H. Li, X.L. Hong, L.N. Ji, X.Y. Li. *J. Inorg. Biochem*., **98**, 423 (2004).
[18] D.F. Xu, S.Z. Ma, Q.Z. He, G.Y. Du. *J. Rare Earths*, **26**, 643 (2008).
[19] B. Yan, Y.S. Song, Z.X. Chen. *Mol. Struct*., **694**, 115 (2004).
[20] J. Easmon, G. Pürstinger, G. Heinisch, T. Roth, H.H. Fiebig, W. Holzer, W. Jäger, M. Jenny, J. Hofmann. *J. Med. Chem*., **44**, 2164 (2001).
[21] M.B. Ferrari, F. Bisceglie, G. Pelosi, P. Tarasconi. *J. Inorg. Biochem*., **98**, 301 (2004).
[22] X.Y. Zhang, S.J. Li, L. Yang. *Chin. J. Inorg. Chem*., **21**, 1109 (2005).
[23] J.T. Groves, I.O. Kady. *Inorg. Chem*., **32**, 3868 (1993).
[24] P. Laine, A. Gourdon, J.P. Launay. *Inorg. Chem*., **34**, 5129 (1995).
[25] T. Ahamad, N. Nishat, S. Parveen. *J. Coord. Chem*., **61**, 1963 (2008).
[26] M.S. Refat, I.M. El-Deen, Z.M. Anwer, S. El-Ghol. *J. Coord. Chem*., **62**, 1709 (2009).
[27] F.M. Belicchi, F. Bisceglie, G. Pelosi. *J. Inorg. Biochem*., **83**, 169 (2001).
[28] V. Arion, K. Wieghardt, T. Weyhermueller, E. Bill, V. Leovac, A. Rufinska. *Inorg. Chem*., **36**, 661 (1997).
[29] M.F. Zhou, Q.Z. He. *J. Rare Earths*, **26**, 473 (2008).
[30] W.J. Geary. *Coord. Chem. Rev*., **7**, 81 (1971).
[31] G.B. Deacon, R.J. Philips. *Coord. Chem. Rev*., **33**, 227 (1980).
[32] M.D. Taylor, C.P. Carte, C.I. Wynter. *Inorg. Nucl. Chem*., **30**, 1503 (1968).
[33] Q.Z. He, S.Z. Ma, D.F. Xu. *Chin. J. Inorg. Chem*., **23**, 1723 (2007).
[34] B.A. Song, S. Yang, Y.P. Hong, G.P. Zhang, L.H. Jin, D.Y. Hu. *J. Fluorine Chem*., **126**, 1419 (2005).
[35] M. Jiang, Y.T. Li, Z.Y. Wu, Z.Q. Liu, C.W. Yan. *J. Inorg. Biochem*., **103**, 833 (2009).
[36] T. Hunter, J. Pines. *Cell*, **79**, 573 (1994).
[37] L.H. Hartwell, M.B. Kastan. *Science*, **266**, 1821 (1994).